Organic & Biomolecular Chemistry

Accepted Manuscript

ROYAL SOCIETY OF CHEMISTRY

www.rsc.org/obc

Journal Name

RSCPublishing

ARTICLE

Induced-fit process through mechanical pivoting of aromatic walls in host-guest chemistry of calix[6]arene aza-cryptands

Cite this: DOI: 10.1039/x0xx00000x

Received 00th January 2012,
Accepted 00th January 2012

DOI: 10.1039/x0xx00000x

www.rsc.org/

Andrea Brugnara[a], Luca Fusaro[b], Michel Luhmer[b], Thierry Prangé[c], Benoit Colasson*[a] and Olivia Reinaud*[a]

The *per-ipso*nitration of a TMPA-capped calix[6]arene has been achieved. The substitution of the six bulky *t*Bu substituents for nitro groups has a strong impact on the behavior of the ligand during guest recognition. The complexation of the aza cap (by H^+ or Cu^+) associated to the encapsulation of a guest triggers an induced-fit process leading to the loss of the cone conformation of the host in favor of alternate conformations. Such a "pivoting" response of one or two walls of the calixarene core induces a large mechanical motion of the corresponding aromatic units. This stands in strong contrast with the "breathing" phenomena previously identified with other calix[6]arene-based complexes that expand or shrink the size of their cone as a function of the guest. Because of the covalently attached rigid TMPA cap, three arene units of this new calixarene host have a restricted mobility, which forces it to respond in a different manner to a supramolecular stress.

Introduction

In natural systems, molecular recognition usually occurs with conformational changes in the structure of the interacting partners. This process, called "induced-fit", has been proposed as a theory to adequately explain experimental evidences not clearly describable assuming a rigid "lock-and-key" model.[1] The way in which molecules recognize and organize themselves via non-covalent interactions is of central interest in supramolecular chemistry as well.[2] Calixarenes,[3] cyclodextrins,[4] resorcinarenes[5] and pillarenes[6] are macrocycles commonly employed in supramolecular chemistry as hosts to bind organic guests. Among these, high-order calix[n]arenes (n ≥ 6) are the more flexible ones and many conformations are possible. The so-called cone conformation is characterized by a well-defined cavity suitable for binding an organic guest, eventhough guest binding was also reported for other conformations.[7, 8, 9, 10, 11, 12]

Some of us have developed several strategies for shaping the calix[6]arene core in this "cavity-offering" conformation: through metal coordination,[13] self-assembly[14] or by covalently connecting three out of the six aromatic units at the small rim.[10, 15] Calix[6]TMPA **1** belongs to the last family of host [Scheme 1; TMPA: tris(2-pyridylmethyl)amine]. This molecule has been widely studied as it acts as a good and polyvalent host for a variety of charged and neutral species.[10, 16] The covalently capped TMPA ligand greatly restricts the conformational freedom of the calixarene core. At the opposite rim of the macrocycle, the substituents (*t*Bu in the parent host defined as compound **1**) also have a strong influence on the hosting properties of the calixarene. They affect the shape of the cavity and they constitute a door that needs to be opened in order to allow a guest to enter or exit. As observed with different calix receptors, it is thus possible to tune the host-guest affinity and the kinetics of the exchange process by removing the bulky *t*Bu substituents at the large rim.[17] Such a modification has also a strong effect on the volume delimited by the calixarene macrocycle and it has been used in the past for other calixarene ligands to encapsulate larger guests.[18] One synthetic strategy is based on a selective *ipso*-nitration, which primarily takes place in *para*-position of the methoxy groups.[19]

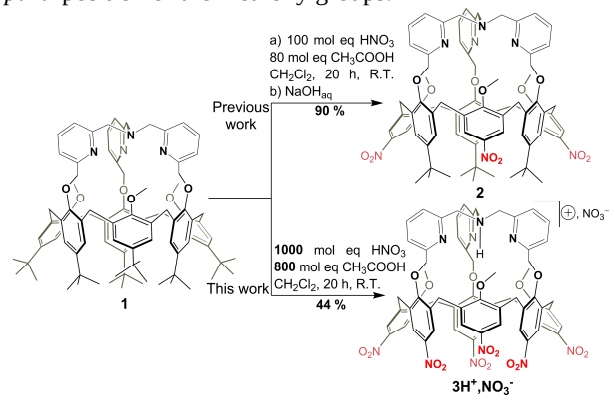

Scheme 1: Synthesis of compounds **2** and **[3·H$^+$,NO$_3^-$]** *via* controlled *ipso*-nitration of the parent calix[6]TMPA **1**.

In the case of calix[6]TMPA, this structural modification has little impact on the host properties because the three *t*Bu groups that close the cavity entrance at the large rim remain unchanged (see compound **2** in Scheme 1). We report herein the *per*-nitration of the calix[6]TMPA ligand (ligand **3**, Scheme 1) and the impact of this substitution pattern on some properties of the macrocycle.

Results and discussion

Synthesis of compounds [3·H$^+$,NO$_3^-$] and 3

During our previous work on the selective *ipso*-nitration of calix[6]TMPA, we noticed that a longer reaction time led to the nitration of a fourth aromatic unit.[19b] This urged us to consider more drastic nitrating conditions in order to achieve *hexa*-substitution. Reaction of **1** with a larger excess of the HNO_3/AcOH mixture (with an [acids]/[calix] ratio ten folds higher than for the previously reported conditions) led to the isolation of a white solid after work-up. The ESMS spectrum (Figure S1) exhibited a single peak and High-Resolution Mass Spectrometry (HRMS) analysis confirmed the nature of the *hexa*-nitrated derivative **3** (found: *m/z* = +1275.3685, calculated: *m/z* = +1275.3696 for [**3**·H$^+$]). Elemental analysis indicated that the mono-protonated species **[3·H$^+$,NO$_3^-$]• [(CH$_3$)$_2$CO]** was the isolated product (44 % yield).

At 300 K in dmso-d_6, several signals of the ^{1}H NMR spectrum of **[3·H$^+$,NO$_3^-$]** exhibit significant broadening (notably the OCH_2 and OCH_3 signals) while the signals of the pyridine units remain rather narrow. Increasing the temperature up to 360 K significantly impacts the spectrum and sharp signals are observed for all the resonances (Figure S3). This behavior indicates the conformational flexibility of the calixarene core (*vide infra*). The ^{1}H NMR spectra recorded in dmso-d_6 at 340 K for **[2·H$^+$,CF$_3$COO$^-$]** and **[3·H$^+$,NO$_3^-$]** present similar profiles, which are compared in Figure 1. [†, §]

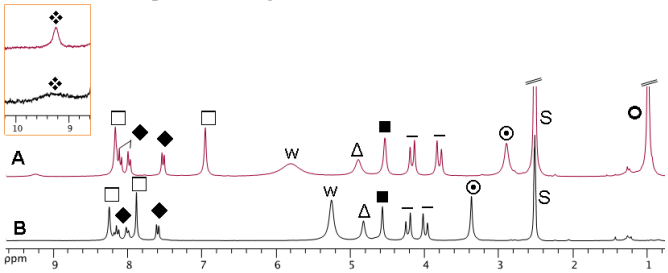

Figure 1: ^{1}H NMR (250 MHz, 340 K, dmso-d_6) spectra of: A) **[2·H$^+$,CF$_3$COO$^-$]**, *i.e.* compound **2** + 3 equivalents of CF_3COOH, B) compound **[3·H$^+$,NO$_3^-$]**. ❖ = NH$^+$, □ = H$_{Ar}$, ◆ = H$_{Py}$, Δ = OCH_2, ■ = NCH_2, – = $ArCH_2$, ⊙ = OCH_3 , O = *t*Bu, w = water, S = solvent.

The absence of resonances in the 0.8-1.3 ppm region of the spectrum of **[3·H$^+$,NO$_3^-$]** clearly indicates the complete substitution of the *t*Bu groups. Both spectra are characteristic of a major, or average, C_{3v}-symmetrical cone conformation. The resonance for the hydrogen atoms of the aromatic units of the calix[6]arene moiety linked to the TMPA cap are downfield shifted ($\Delta\delta H_{Ar}$ = +0.92 ppm) due to the presence of the electron-withdrawing nitro groups instead of the *t*Bu substituents in **2**. The resonance for the methoxy groups of **[3·H$^+$,NO$_3^-$]**, compared to the one for **[2·H$^+$,CF$_3$COO$^-$]**, is downfield shifted ($\Delta\delta_{OCH3}$ = +0.47 ppm), suggesting that these groups point out of the cavity on average. In strong contrast with the *hexa*-*t*Bu compound **1**, the ^{1}H NMR spectrum of the *hexa*-nitrated derivative **[3·H$^+$,NO$_3^-$]** was found to be strongly dependent on the temperature. This difference is due to the presence in **1** of bulkier *t*Bu substituents which reduce the conformational freedom of the macrocycle. This is also observed in the two spectra recorded at 300 K in acetone-d_6 (Figure S5). The resonances of the protons on the anisyl moieties are much broader for **[3·H$^+$,NO$_3^-$]** than for **[1·H$^+$,NO$_3^-$]**.

Characterization of [3·H$^+$,NO$_3^-$] in the solid state

Single crystals suitable for X-Ray Diffraction (XRD) analysis were grown at 298 K by slow solvent evaporation of a solution of **[3·H$^+$,NO$_3^-$]** in acetone (Figure 2).

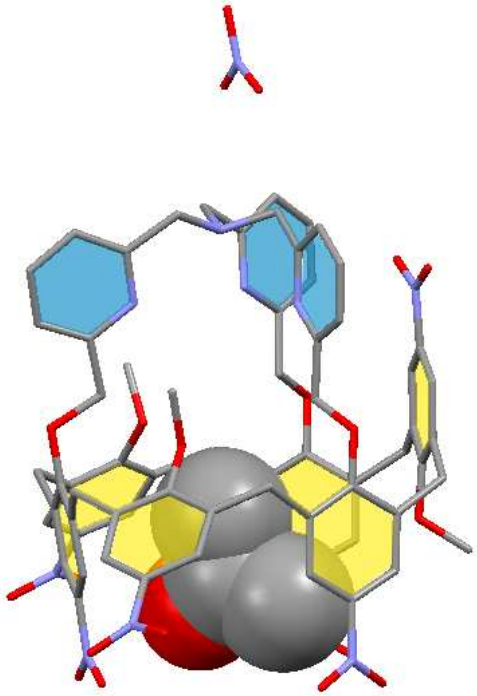

Figure 2: XRD structure of [**3**·H$^+$,NO$_3^-$]. Hydrogen atoms have been omitted for clarity. Color code for the atoms: grey = carbon, blue = nitrogen, red = oxygen. The acetone molecule is depicted in space filling representation.

The presence of a nitrate anion in the structure confirms the mono-cationic nature of the host. The XRD structure of **[3·H$^+$,NO$_3^-$]** shows that the calix[6]arene macrocycle is in a partial cone conformation and has a C_s symmetry. The plane of the upside down aromatic unit is almost parallel to the closest pyridine unit of the TMPA cap. The shortest nitro-*O*···ring centroid distance is 3.22 Å. This distance is at the very limit of the combined van der Waals radii of a carbon and oxygen

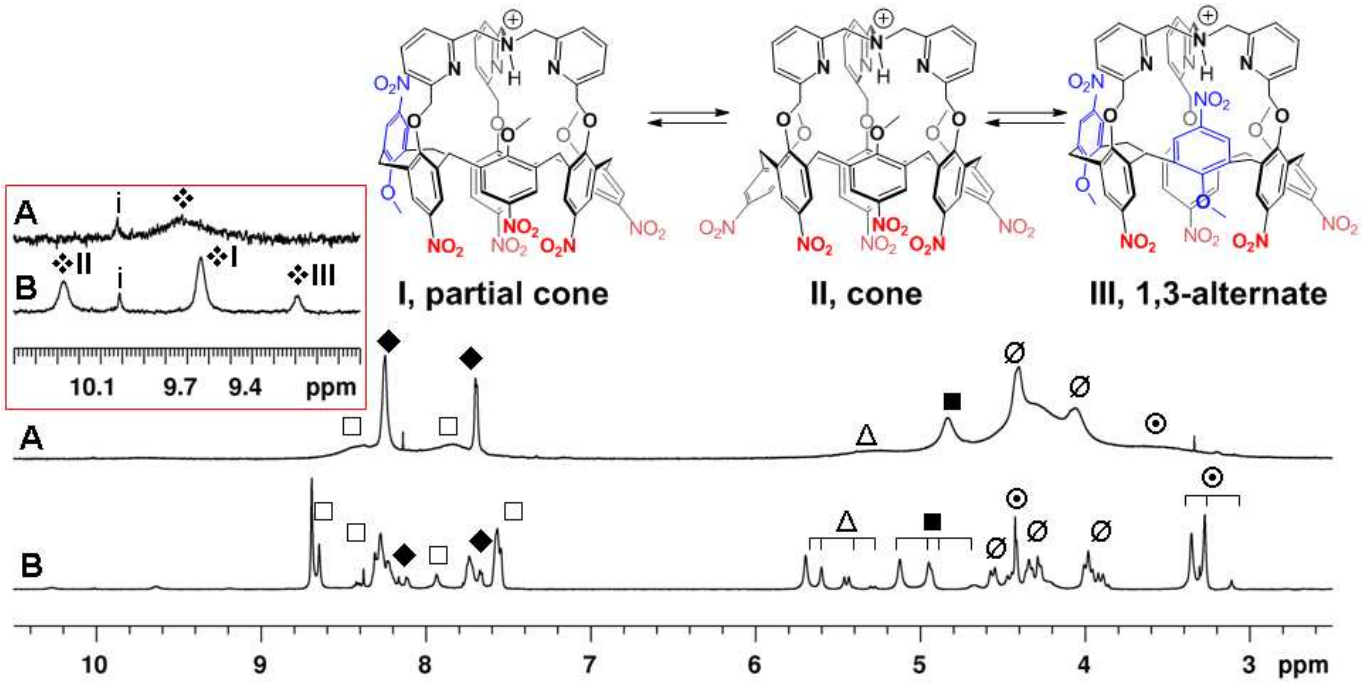

Figure 3: ^{1}H NMR (600 MHz, acetone-d_6) spectra of **[3·H$^+$,NO$_3^-$]**: A) at 300 K B) at 238 K. ❖ = NH$^+$ (i = impurity), □ = H_{Ar}, ◆ = H_{Py}, Δ = OCH_2, ■ = NCH_2, Ø = $ArCH_2$, ⊙ = OCH_3; and representation of the three different conformers **I**, **II** and **III** in equilibrium (the acetone guest has been omitted for clarity).

atoms (3.22 Å)[20] and suggests the presence of a nitro-π interaction.[21] The cavity is filled with a molecule of acetone that points its dipole towards the large rim of the calix[6]arene core. The orientation of the acetone guest molecule is different from what has been previously observed in a highly polarized calixarene receptor having a polycationic cap. In that case, the strong charge-dipole interaction directs the dipole moment of the guest molecule along the C_3 axis of the calixarene.

Having evidenced a solid state structure with a partial cone conformation, and having noticed the relatively high mobility of the calixarene core in solution above RT, we decided to explore its conformational behavior at lower temperatures, in the same solvent as the one out of which the XRD structure has been obtained.

Conformational analysis of [3·H$^+$,NO$_3^-$] in acetone solution

In order to identify the putative species in equilibrium, NMR analyses were conducted at lower temperatures in acetone-d_6. The ^{1}H NMR spectrum of **[3·H$^+$,NO$_3^-$]** recorded in acetone-d_6 at 300 K also presents relatively broad resonances but the overall signature still corresponds to an average C_{3v} symmetry (Figure 3, spectrum A). However, at lower temperatures, new profiles with additional resonances were obtained (Figure S6), attesting to the presence of several conformers in slow exchange on the spectroscopic timescale. The ^{1}H NMR recorded at 600 MHz and 238 K is displayed in Figure 3 (spectrum B).

In-depth analyses of 1D and 2D NMR spectra recorded at 238 K and 600 MHz reveal the presence of three different conformations. Each of them could be unambiguously identified (Figure 4 and SI for the full description of the NMR experiments and deconvolution procedure): the major conformation (**I**: 54 %) corresponds to a partial cone conformation with one unit being flipped upside down (C_s symmetrical pattern), the second species (**II**: 33 %) corresponds to a flattened-cone conformation (C_{3v} symmetrical pattern), and a last species (**III**: 13 %) has a 1,3-alternate conformation (C_s symmetrical pattern). The ratio between the different conformations are significantly temperature dependent (see SI). The proportion of the cone conformation increases at low temperature. The ratio between the two major conformers (cone **II** *vs* partial cone **I**) is 0.62 at 238 K and reaches 1 at about 205 K. Hence, the major conformer in acetone above 205 K corresponds to the partial cone conformation adopted in the solid state. A van't Hoff plot for the equilibria allowed an estimation of the thermodynamic parameters estimated for the inversion of one p-nitroanisol unit. For the **II**(C_{3v}) ⇆ **I**(C_s) equilibrium, $\Delta H°$= 5.9 ±0.6 kJ mol^{-1} and $\Delta S°$= 29 ±3 J K^{-1} mol^{-1}. For the second inversion, i.e. for the **I**(C_s) ⇆ **III**(C_s) equilibrium, they were estimated to be $\Delta H°$= 7.3 ±0.6 kJ mol^{-1} and $\Delta S°$= 19 ±3 J K^{-1} mol^{-1}. These values show that the C_{3V} species is enthalpically favored and the inversion of the anisol units is an entropically driven process. The positive entropy value likely reflects a higher number of microstates for the C_s conformations.[Ω]

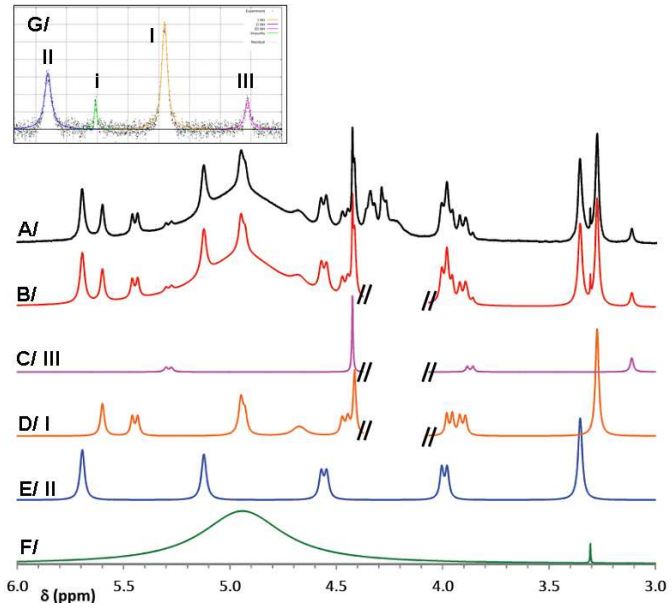

Figure 4: Deconvolution analysis of the ^{1}H NMR spectrum of **[3·H$^+$,NO$_3^-$]**. A) Experimental spectrum (600 MHz, acetone-d_6, 238 K); B) Sum of the individual contributions; C) Deconvoluted spectrum of conformation **III**; D) Deconvoluted spectrum of conformation **I**; E) Deconvoluted spectrum of conformation **II**; F) Deconvoluted spectrum of the water and methanol contributions; G) Deconvolution of the NH$^+$ region (i = impurity).

Conformational analysis of 3 in acetone solution

The neutral form of ligand **3** was obtained by reacting **[3·H$^+$,NO$_3^-$]** with an excess of K_2CO_3 in acetonitrile. After filtration and evaporation of the solvent, **3** was isolated quantitatively. The ^{1}H NMR spectrum of **3** dissolved in acetone-d_6 at 300 K shows sharp resonances, which only slightly broadened at 240 K (Figure 5). In contrast to the protonated compound, the overall profile of the spectra remained characteristic of a C_{3V} symmetry even at very low T and no extra peak attesting to the presence of *Cs* conformers could be observed. Interestingly also, the δ shift variation of the aromatic protons as a function of the temperature indicates that the molecule switches from a straight cone conformation to a flattened cone conformation. Such a well-known behavior indicates inclusion of the solvent inside the cavity at low T.

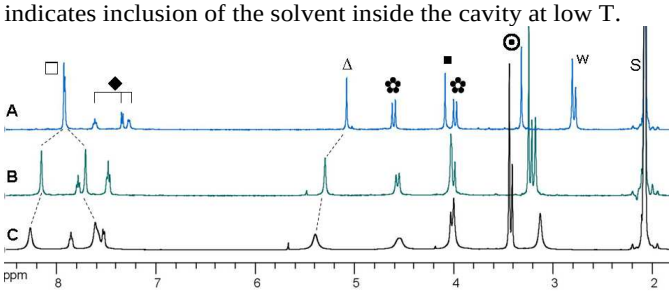

Figure 5: ^{1}H NMR (500 MHz, acetone-d^6) of **3**: A) 300K; B) 260K; C) 240K;. □ = H_{Ar}, ◆ = H_{Py},.,Δ = OCH_2, ■ = NCH_2, ✿ = $ArCH_2$, ⊙ = OCH_3, w = water, S = solvent

Hence, the comparative solution analyses of **3** and **[3·H$^+$,NO$_3^-$]** in acetone have evidenced different conformational properties: the presence of a proton in the TMPA cap, somehow, stabilizes alternate conformations. Wanting to know whether the nature of the guest has an impact too, we studied the corresponding copper(I) complex with two different well-identified guests inside the macrocycle.

Conformational behavior of cuprous complexes with various guests

The cuprous complex was prepared *in situ* by mixing equimolar amounts of **3** and **Cu(CH$_3$CN)$_4$B(C$_6$F$_5$)$_4$**[22] in acetone-d_6, and characterized by ^{1}H NMR spectroscopy. At 300 K, the ^{1}H NMR spectrum of **[Cu^{I}3(CH$_3$CN)]B(C$_6$F$_5$)$_4$** showed broad resonances and no signal in the up-field region could be detected (Figure S21). This is very different from the behavior of the cuprous complex of **1** for which the presence of sub-stoichiometric traces of acetonitrile in the medium led to the emergence of a sharp peak at ca. –1 ppm corresponding to the quantitative inclusion of CH_3CN.[16b] In the case of **3**, the singlet relative to the presence of 4 equivalents of CH_3CN is slightly broad and up-field shifted (Δδ= –0.14 ppm). This last observation suggests a fast "*in-out*" exchange for the nitrilo-guest on the spectroscopic timescale.

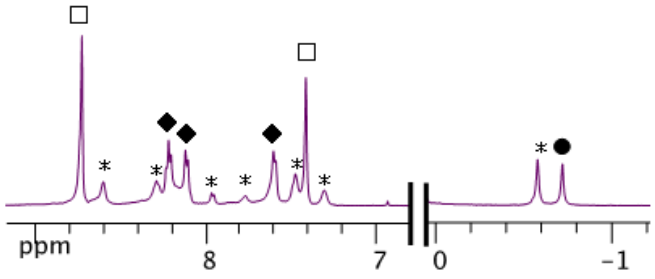

Figure 6: Aromatic and up-field regions for the ^{1}H NMR (500 MHz, acetone-d_6, 240 K) spectrum of **[Cu^{I}3(CH$_3$CN)]B(C$_6$F$_5$)$_4$**. □ = H_{Ar}, ◆ = H_{Py}, ● = CH_3CN_{in}, * = *Cs* conformations.

The ^{1}H NMR spectrum was completely different at low temperature, presenting sharper resonances (Figure 6). A careful analysis (see the SI) in the region of the aromatic protons evidenced the presence of the exact same three conformers as in the case of **[3·H$^+$,NO$_3^-$]**. In the case of the cuprous complex however, the ratio between the partial cone, cone and 1,3-alternate conformations at 260 K was 47 % / 41 % / 12 %, respectively (Figure 8). Two singlets at around δ = –0.6 ppm attested to the inclusion of CH_3CN in the calixarene cavities that is in a slow exchange regime, which was confirmed by saturation transfer experiments (Figure S22). These peaks globally integrated for ca. 60 % and 40 % of one guest equivalent, very probably due to signal overlapping for the major and minor conformers.

We then tested the coordination of a larger guest molecule and analyzed the consequences of its recognition on the distribution of the conformers. When 15 equivalents of benzonitrile were added to the *in situ* prepared solution of **[Cu^{I}3(CH$_3$CN)]B(C$_6$F$_5$)$_4$**, spectral changes revealed the substitution of CH_3CN by PhCN in the calixarene cavity (Figure 7 and Figure S24).

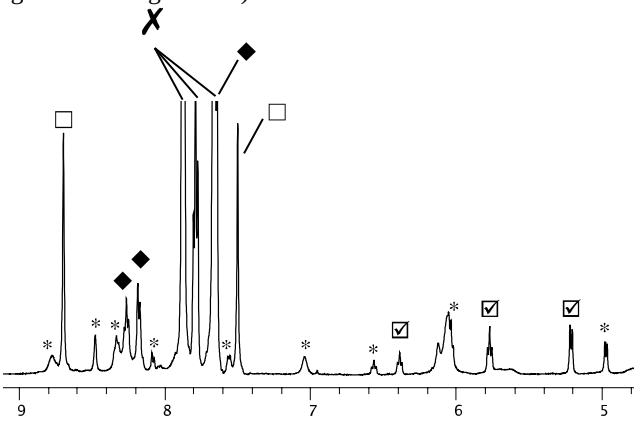

Figure 7: Aromatic region of the ^{1}H NMR (500 MHz, acetone-d_6, 240 K) spectrum of **[Cu^{I}3(PhCN)]B(C$_6$F$_5$)$_4$**. □ = H_{Ar}, ◆ = H_{Pys}, ✗ = $PhCN_{out}$, ☑ = $PhCN_{in}$, * = C_s conformation.

Indeed, the two singlets at –0.58 ppm and –0.72 ppm disappeared, attesting to the absence of CH_3CN_{in}, i.e. its replacement by another guest molecule. In the region between 4.8 and 6.6 ppm, two sets of signals appeared, each of them attributed to a PhCN molecule. Both are up-field shifted compared to free PhCN (major conformation: Δδ(H*o*) = –2.66 ppm, Δδ(H*m*) = –1.89 ppm, Δδ(H*p*) = –1.40 ppm; minor conformation: Δδ(H*o*) = –2.90 ppm, Δδ(H*m*) = –1.63 ppm, Δδ(H*p*) = –1.23 ppm), which indicates that they stand for PhCN sitting in the heart of the calixarene cavity. From this experiment, the equilibrium constant for the displacement of CH_3CN by PhCN at 240 K can be estimated to be higher than 6. Once again, this behavior is markedly different from the parent cuprous complex based on **1**. Indeed, the stability of **[Cu^{I}1(CH$_3$CN)]PF$_6$** is so high that a large excess of PhCN (> 30 equiv.) does not displace an acetonitrile guest stoechiometrically bound. The *t*Bu-decorated macrocycle defines a cavity that perfectly fits to the size of CH_3CN, and its rigidity disfavors the distortion necessary to stabilize PhCN in its heart.[16] The analysis of the more intense signals for the host and encapsulated guest indicate that the ligand adopts two different conformations: the major one (in a 63 % ratio) is C_{3v} symmetrical while the minor one (37 %) has a lower degree of symmetry. This last observation highlights the flexibility of the *hexa*-nitrated host, which can adjust its conformation depending on the structure/size of the encapsulated guest.

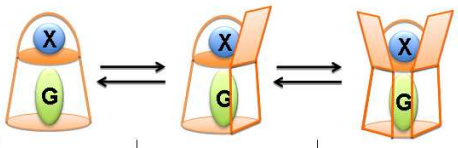

X	G			
Ø	$(CH_3)_2CO$	100 %		
H^+	$(CH_3)_2CO$	33 %	54 %	13 %
Cu^+	CH_3CN	41 %[a]	47 %[a]	12%[a]
Cu^+	PhCN	63 %	37 %	

Figure 8: Percentages of the different conformers measured at 240 K in acetone as a function of the presence of a cation **X** in the cap and a guest **G** in the cavity. [a] the ratio was measured at 260 K.

Discussion

These data reveal that the conformational properties of the calix[6]arene derivatives that are capped by a TMPA unit are strongly influenced not only by the substitution pattern at the large rim, but also by the state of the aza cap (empty/protonated/metallated) and the nature of the guest. Whereas both neutral and protonated species very probably host a solvent molecule, at least at low T, it is reasonable to state that protonation itself induces such conformational changes. This is consistent with the fact that an 1,3-alternate conformation was also characterized in the solid state for **[1·H$^+$,ClO$_4^-$]** without any guest in the calixarene cavity.[10] An induced-fit through guest-binding was observed with the cuprous complex of **3**. While an acetonitrile molecule guest favors the C_s symmetrical structures of the calixarene (59 % *vs*. 41 % for the C_{3v} complex), its substitution for benzonitrile inverts the ratio (37 % for the C_s symmetry *vs*. 63 % for the C_{3v} symmetry) (Scheme 2B). This pivoting process strongly differs from the usual induced-fit process observed in most of the calix[6]arene receptors that we have previously studied. Depending on the link that connects three aromatic units in alternate position at the small rim, the degree of freedom left to the three others differs. As a result, the induced fit process allowing the calix[6]arene host to adapt to its guest(s) is either breathing or pivoting (see Scheme 2). With three imidazole bound to a metal ion [typically Zn(II) or Cu(I/II)] or with the flexible TREN hat [TREN: tris(2-aminoethyl)amine], the connected aromatic units (colored in red in scheme 2A) are in *out* position relative to the others. Hence, breathing through the more flexible anisole units (yellow) allows the host to expand (with dimethyl dopamine as a guest for example) or shrink (with a water molecule or CO as a guest) the space available for the guest through partial inclusion of an aromatic unit in the cavity.[13,15] With ligand **3** bearing a rigid TMPA hat, the connected aromatic units (colored in red in scheme 2B) are in *in* position relative to the others. Hence breathing is disfavored and pivoting of the anisole units (yellow) becomes

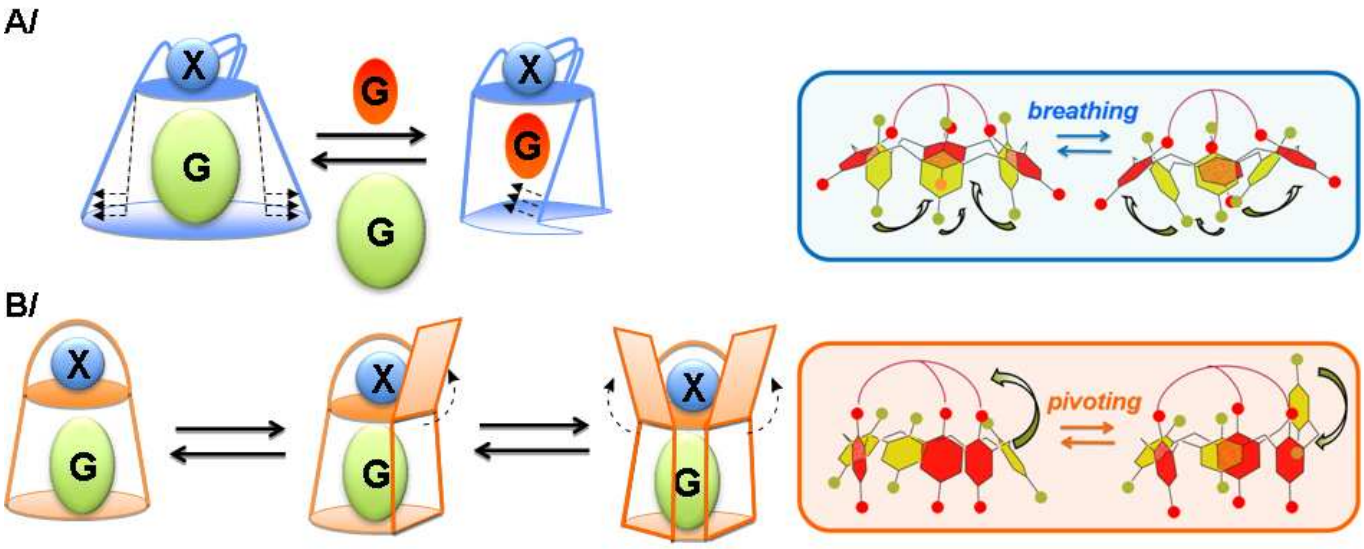

Scheme 2. Induced fit as observed with A/ calix[6]tris(imidazole) and TREN-based Cu and Zn complexes**,** B/ with the calix[6]TMPA-based complexes described in the article upon the encapsulation of a guest (**G** = RNH_2, ROH, RCN, CO; **X** = Zn^{2+}, $Cu^{+/++}$ or H^+). In the boxes, the conformations of capped calix[6]arenes are schematized according to DRX structures (see ref in the text).

the major adaptative process, induced by either cation hosting in the hat (H^+ or Cu^+) and/or binding an organic guest in the cone (acetone, CH_3CN, PhCN).

Conclusion

We have here reported a simple synthetic procedure that allows, for the first time, the *per*-nitration of the calix[6]arene large rim of a poly-aza ligand. The replacement of all six *t*Bu substituents of calix[6]azacryptand **1** by NO_2 groups was cleanly achieved by strengthening the acidic conditions of the reaction of nitration and the corresponding *hexa*-nitrated derivative **[3·H^+,NO_3^-]** was isolated in a moderate yield. This stands in strong contrast with all other calix-aza ligands previously studied, which underwent either only *tri*-nitration or degradation of the aza core at the small rim under the same experimental conditions. These different behaviors may be ascribed to the particular rigidity and geometry of the TMPA-capped calixarene cores: the simultaneous protonation of the pyridine units facing each other is disfavored by the geometrical constrains at the small rim, and the related deactivation process towards nitration is not as effective as for the more flexible aza-ligands.

The structural changes at the large rim – six small NO_2 groups in **3** instead of six bulky, electron-donating *t*Bu groups in **1** – have a major impact on the flexibility of the macrocycle. Indeed, such a modification confers new adaptive properties to the cavity that can undergo important geometrical changes depending on the size/shape of the guest and cation-binding in the TMPA cap. In-depth solution NMR analyses revealed that, depending on the conditions, the calixarene core can adopt various conformations, one of which was characterized by XRD. They also allowed identifying and quantifying unambiguously the nature of the alternate conformers present in solution.

In the case of the cuprous complex, an "induced fit" process has been unambiguously characterized. Such flexibility is identified by the upside-down flipping of one or two anisole moieties. Hence, in strong contrast to all previously related calix[6]arene-based metal complexes that undergo a breathing motion as an induced-fit response (Figure 2), host **1** undergoes pivoting one or two aromatic walls. This is attributable to the different capping systems, the TMPA cap constraining and rigidifying the three connected aromatic units in endo position. Interestingly, such a conformational change results in a large mechanical motion, although induced by a relatively small chemical stress. Finally, it is worth noting that the large rim hexa-substitution of compound **1** also opens the route for the introduction six functional groups at the small rim. We are now exploring the possible exploitation of such a mechanical response and functionalization pattern for the conception of new devices. [23]

Experimental section

General experimental methods

CH_2Cl_2 was dried over CaH_2 and distilled under argon atmosphere. Other solvents and chemicals were of reagent grade and were used without further purification. **^{1}H** and **^{13}C NMR** spectra were recorded on a Brucker ARX (250 MHz) spectrometer or an Advance 500 spectrometer and Varian *(part of Agilent)* VNMRS spectrometer operating at 14.1 T (599.94 MHz for ^{1}H and 150.87 MHz for ^{13}C). Chemical shifts are

expressed in ppm. **MS** (**ESI**) analyses were obtained with a ThermoFinnigen LCQ Advantage spectrometer using methanol as solvent. **HRMS** and **Elemental Analysis** were performed at the "Institut de Chimie des Substances Naturelles", Gif-sur-Yvette, France. **IR** spectra were obtained with a Perkin-Elmer Spectrum on FTIR spectrometer equipped with a MIRacleTM single reflection horizontal ATR unit (germanium crystal). XRD diffraction data were recorded at the European Synchrotron Facility (ESRF, Grenoble), beam line BM30A (FIP). The wavelength was set to 0.865 Å and the detector was an ADSC Quantum 315r. The temperature of the crystal was maintained at 100 K during data collection.

Synthesis of [3·H$^+$,NO$_3^-$]. Compound **1** (120 mg, 8.9 10^{-2} mmol) was reacted in distilled CH_2Cl_2 (12 mL) with an HNO_3/AcOH mixture (8.0 mL, 1:1, v/v). The reaction was monitored by ESI-MS (CH_3OH). Once the reaction appeared complete (ca. 20h) the system was diluted with 20 mL of CH_2Cl_2 and a white solid was collected by filtration and washed with dichloromethane. The solid was dissolved in acetone and precipitated with water. After filtration, **[3·H$^+$,NO$_3^-$]** was isolated as a white solid (50 mg). The elemental analysis indicated the presence of one acetone molecule per calixarene molecule.

Yield: 44%. **Elemental Analysis:** found: C, 57.74 %; H, 4.41 %; N, 10.51 %; calcd for **[3·H$^+$,NO$_3^-$].(H$_2$O)$_2$.[(CH$_3$)$_2$CO]** C, 57.86 %; H, 4;57 %; N, 10.76 %. **mp:** > 260°C. **IR (solid):** υ = 2958, 1605, 1582, 1522, 1461, 1346, 1264, 1218, 1096 cm^{-1}. **HRMS:** calc. for $C_{66}H_{55}N_{10}O_{18}$ **[3·H$^+$]** 1275.3696; found 1275.3685. **^{1}H NMR** (250 MHz, dmso-d_6, 360 K): δ = 8.18 (s, 6H, H_{Ar}), 8.12 (t, 3H, H_{Py}), 7.95 (d, 3H, H_{Py}), 7.92 (s, 6H, H_{Ar}), 7.58 (d, 3H, H_{Py}), 4.80 (s, 6H, OCH_2), 4.57 (s, 6H, NCH_2), 4.23 (d, 6H, $ArCH_2$ax, J = 15 Hz), 3.98 (d, 6H, $ArCH_2$eq, J = 15 Hz), 3.36 (s, 9H, OCH_3). **^{13}C NMR** (62.5 MHz, dmso-d_6, 300 K): δ = 162.35, 158.58, 156.76, 149.37, 143.80, 143.39, 139.60, 134.18, 134.07, 127.24, 124.18, 123.40, 120.16, 74.41, 61.32, 56.54, 29.87 ppm.

Synthesis of 3. 3 is prepared by reacting **[3·H$^+$,NO$_3^-$]** with an excess of K_2CO_3 (30 eq) in acetonitrile. After stirring the heterogeneous solution overnight, the excess of K_2CO_3 is removed by filtration and washed with acetonitrile. The organic phase is evaporated to quantitatively afford **3** as a yellow solid.

^{1}H NMR (250 MHz, dmso-d_6, 300 K): δ = 7.97 (s, 6H, H_{Ar}), 7.82 (s, 6H, H_{Ar}), 7.72 (t, 3H, H_{Py}), 7.35 (m, 6H, H_{Py}), 5.09 (s, 6H, OCH_2), 4.39 (d, 6H, $ArCH_2$ax, J = 15 Hz), 3.93 (m, 6H, $ArCH_2$eq + NCH_2), 3.05 (s, 9H, OCH_3).

Acknowledgements

This project was supported by the CNRS (Institut de Chimie), the Ministère de l'Enseignement Supérieur et de la Recherche and the Agence Nationale pour la Recherche [Cavity-zyme(Cu) Project ANR-2010-BLAN-7141].

Notes and references

[a] Laboratoire de Chimie et de Biochimie Pharmacologiques et Toxicologiques, CNRS UMR 8601, PRES Sorbonne Paris Cité, Université Paris Descartes, 45 rue des Saints Pères, 75006 Paris, France. E-mail: benoit.colasson@parisdescartes.fr; olivia.reinaud@parisdescartes.fr.

[b] Laboratoire de Résonance Magnétique Nucléaire Haute Résolution, Université Libre de Bruxelles, Avenue F.D. Roosevelt 50, CP160/08, B-1050 Brussels, Belgium.

[c] Laboratoire de Cristallographie et de Résonance Magnétique Nucléaire Biologiques, CNRS UMR 8015, Université Paris Descartes, 4, Avenue de l'Observatoire, 75006 Paris, France.

† The nature of the counter-anion has no significant influence on the ^{1}H NMR spectrum.

§ The spectrum of **2** was recorded in the presence of three equivalents of trifluoroacetic acid. Under these conditions, the TMPA cap is monoprotonated. See ref 9.

Ω At very low temperature, another dynamic process was detected for the partial cone conformation but could not be identified.

Electronic Supplementary Information (ESI) available: [ESI-MS spectra, 1D, 2D and VT NMR experiments, deconvolution analysis and XRD data]. See DOI: 10.1039/b000000x/

1 J. A. Yankeelov, D. E. Koshland *J. Biol. Chem.* 1965, **204**, 1593-1602.
2 J. M. Lehn, *Supramolecular Chemistry*, 1995, VCH: Weinheim.
3 (a) C. D. Gutsche, in *Calixarenes An introduction*, Monographs in: Supramolecular Chemistry, (Ed: J. F. Stoddart, The Royal Society of Chemistry, Cambridge), 2nd edn, 2008; (b) C. D. Gutsche, in *Calixarenes Revisited*, Monographs in: Supramolecular Chemistry, (Ed: J. F. Stoddart, The Royal Society of Chemistry, Cambridge), 1998.
4 J. Szejtil *Chem. Rev.* 1998, **98**, 1743-1753.
5 P. Timmerman, W. Verboom, D. N. Reinhoudt *Tetrahedron* 1996, **8**, 2663-2704.
6 (a) T. Ogoshi, S. Kanai, S. Fujinami, T. Yamagishi, Y. Nakamoto *J. Am. Chem. Soc.* 2008, **130**, 5022-5023; (b) H. Li, D.-X. Chen, Y.-L. Sun, Y. B. Zheng, L.-L. Tan, P. S. Weiss, Y.-W. Yang *J. Am. Chem. Soc.* 2013, **135**, 1570-1576.
7 M. Ménand, A. Leroy, J. Marrot, M. Luhmer, I. Jabin *Angew. Chem. Int. Ed.* 2009, **48**, 5509-5512.
8 Y. Chen, Y. Chen *Tetrahedron Lett.* 2000, **41**, 9079-9082.
9 K.-C. Chung, K.-S. Song, K. N. Kim, J. Cho, S.-K. Chang, S. Ahn *Bull. Korean Chem. Soc.* 2007, **28**, 1871-1873.
10 X. Zeng, D. Coquière, A. Alenda, E. Garrier, T. Prangé, Y. Li, O.Reinaud, I. Jabin, *Chem. Eur. J.* 2006, **12**, 6393-6402.
11 P. Neri, M. Foti, G. Ferguson, J. F. Gallagher, B. Kaitner, M. Pons, M. A. Molins, L. Giunta, S. Pappalardo *J. Am. Chem. Soc.* 1992, **114**, 7814-7821.
12 A. J. Petrella, N. K. Roberts, D. C. Craig, C. L. Raston, R. N. Lamb *Chem. Commun.* 2003, 1014-1015.
13 D. Coquière, S. Le Gac, U. Dabrost, O. Sénèque, I. Jabin, O. Reinaud *Org. Biomol. Chem.* 2007, **7**, 2485-2500.
14 S. Le Gac, M. Luhmer, O. Reinaud, I. Jabin *Angew. Chem. Int. Ed.* 2006, **45**, 3123-3126.

15 (a) U. Darbost, M.-N. Rager, S. Petit, I. Jabin, O. Reinaud *J. Am. Chem. Soc.* 2005, **127**, 8517-8525; (b) G. Izzet, M-N. Rager, O. Reinaud *Dalton Trans* 2007, 771-780.
16 (a) G. Izzet, X. Zeng, H. Akdas, J. Marrot, O. Reinaud *Chem. Commun.* 2007, 810-812; (b) G. Thiabaud, G. Guillemot, I. Schmitz-Afonso, B. Colasson, O. Reinaud *Angew. Chem. Int. Ed.* 2009, **48**, 7383-7386.
17 Y. Rondelez, M.-N. Rager, A. Duprat, O. Reinaud *J. Am. Chem. Soc.* 2002, **124**, 1334-1340.
18 D. Coquière, J. Marrot, O. Reinaud *Org. Biomol. Chem.* 2008, **6**, 3930-3934.
19 (a) S. Redon, Y. Li, O. Reinaud *J. Org. Chem.* 2003, **68**, 7004-7008; (b) M. Lejeune, J.-F. Picron, A. Mattiuzzi, A. Lascaux, S. De Cesco, A. Brugnara, G. Thiabaud, U. Darbost, B. Colasson, O. Reinaud, I. Jabin *J. Org. Chem.* 2012, **77**, 3838-3845.
20 A. Bondi, *Phys. Chem.* 1964, **68**, 441-451.
21 (a) D. A. Parrish, J. R. Deschamps, R. D. Gilardi, R. J. Butcher *Crystal Growth Des.* 2008, **8**, 57-62; (b) J. R. Deschamps, D. A. Parrish, R. J. Butcher *NRL Review,* 2008, 71-77; (c) L. Huang, L. Massa, J. Karle, *Proc. Natl. Acad. Sci. USA* 2008, **105**, 13720-13723.
22 For the synthesis of **$Cu(CH_3CN)_4B(C_6F_5)_4$** see: H.C. Liang, E. Kim, C. D. Incarvito, A. L. Rheingold, K. D. Karlin *Inorg. Chem.* 2002, **41**, 2209-2212.
23 A. Mattiuzzi, I. Jabin, C. Mangeney, C. Roux, O. Reinaud, L. Santos, J.-F. Bergamini, P. Hapiot, C. Lagrost *Nat. Comm.* 2012; DOI: 10.1038/ncomms2121.